

# A Biomechanical Analysis of the Causes of Traumatic Brain Injury in Infants and Children

Werner Goldsmith, PhD\* and John Plunkett, MD†

**Abstract:** There is significant disagreement among medical professionals regarding the mechanisms for infant brain injury. This disagreement is due in part to the failure by some to acknowledge and incorporate known biomechanical data and models into hypotheses regarding causes. A proper biomechanical understanding of the mechanisms of traumatic brain injury (TBI) challenges many published and testified assumptions regarding TBI in infants and children.

This paper analyzes the biomechanical relationship between the causes of TBI in infants and children, and their physiological consequences. Loading characteristics, injury parameters and criteria, scaling, failure characteristics, differences between infants and adults, and impact due to falls are described and discussed in the context of the laws of mechanics. Recent studies are critiqued with reference to their contribution to an understanding of brain injury mechanisms. Finally, methods for improving our currently incomplete knowledge of infant head injuries, and their mechanisms, consequences and tolerances are proposed. There is an urgent need for close collaboration between physicians and biomechanicians to objectively and scientifically evaluate infant head injuries to further define their mechanical bases, and to assist in their diagnosis and treatment.

**Key Words:** Traumatic Infant Head Injury, Shaken Baby Syndrome (SBS), Impact, Impulsive Loading

(*Am J Forensic Med Pathol* 2004;25: 89–100)

**B**iomechanicians and physicians evaluate trauma in fundamentally different ways. A biomechanician constructs or accepts a particular system, obtains its physical and geometric characteristics, applies a specified and quantifiable input (load), and then determines the output using experimental,

analytical, and numerical techniques. A physician sees the end product of signs and symptoms, and relies primarily if not exclusively on experience and observational case material to diagnose and treat. A biomechanician traces a continuous path from cause to effect using the laws of nature, tries to determine the specific mechanism of an injury, and attempts to either establish or eliminate an ultimate mechanical cause. A physician treats the physiological alterations due to an injury, and does not usually need to validate the diagnosis with a controlled experiment prior to making a decision to initiate treatment.

Recent advances in the quantitative characterization of the material and structural properties of the developing infant brain and skull permit the biomechanician to study the differences between traumatic brain injury in infants and adults.<sup>1–6</sup> The findings suggest that understanding the unique age-dependant properties of the developing brain and skull is critical for determining both impulsive and impact loading thresholds. New and continued research, including pediatric injury models, will play a vital role in evaluating infant traumatic head injury.<sup>7</sup> Collaboration between biomechanicians and physicians will provide a foundation for developing improved clinical, diagnostic, preventive, therapeutic, and rehabilitative strategies to address the unique problems of pediatric head injury.

## Biomechanics

*Biomechanics* is the application of the science of mechanics to biologic systems, whether plant or animal.<sup>8,9</sup> *Mechanics* is defined as the consequences of the application of forces and couples (a set of equal, parallel and oppositely directed forces) to one object or a system of objects (solid, liquid or gas). A solid object may be considered analytically as a particle (a point in space that has mass, and that resists motion); as a group or system of such particles; or as a single solid body that may be either rigid or deformable.

Skull and brain motion and the forces causing them are governed by Newton's Second Law, Force = mass times acceleration ( $F = ma$ ). The displacement of the head (as an object with mass) can be described as planar or as occurring in space as defined by motion in one or all 3 of the X-, Y-, and Z-axes. The displacements are governed by Newton's Law

From the \*Graduate School, Departments of Mechanical Engineering and Bioengineering, University of California, Berkeley, California; and the †Department of Laboratory and Medical Education, Regina Medical Center, Hastings, Minnesota.

Reprints: John Plunkett, MD, Laboratory and Medical Education Director, Regina Medical Center, 1175 Nininger Road, Hastings, MN 55033.

E-mail: plunkettj@reginamedical.org.

Copyright © 2004 by Lippincott Williams & Wilkins

ISSN: 0195-7910/04/2502-0089

DOI: 10.1097/01.paf.0000127407.28071.63

and constraints, and can be extended to provide an impulse-momentum and a work-energy relation. The neck is a constraint to this motion.

**Loading characteristics**

Traumatic brain injury (TBI) in infants, children and adults is caused by one of 2 mechanisms: (a) *Impulsive Loading*, when the head moves as the result of motion imparted to some other part of the body (“whiplash”, Figs. 1a and 1b); and (b) *Impact Loading*, where the head either strikes a stationary object (Fig. 2a) or is struck by a moving object (Fig. 2b). These events are mechanically distinct and separate and they have different consequences. Both actions cannot occur simultaneously, although they may happen sequentially.

Impulsive loading of an unsupported head will cause it to rotate about some point of the cervical spine, from the occipital condyles to C7/T1. In such a rotation, the skull will move at a different rate from the brain, which lags behind because the brain and skull are not rigidly linked and force is transmitted to the skull prior to the brain, in the same way that a car responds to an impact before a passenger. This differential displacement may produce tensile failure of the bridging veins, which occurs on the average when they are stretched 30% beyond unloaded length.<sup>10,11</sup> Further, at a given input, injury due to impulsive loading typically decreases from the cortex towards the base of the brain.<sup>12,13</sup> There are also regional and directional differences of brain injury type and distribution from impulsive loading, and differences due to vessel orientation.<sup>14–16</sup> Sagittal plane acceleration at sufficient magnitude usually causes a subdural hematoma (SDH), while coronal plane acceleration at sufficient magnitude usually results in traumatic axonal injury (TAI, which may be focal or diffuse [DAI]).<sup>17</sup> Most studies have used a single applied load, but a recent investigation of repetitive loading of rats showed increasing damage with successive load application after significant periods of quiescence.<sup>18</sup>

Impact, in contrast, is the collision of 2 solid objects at a velocity sufficient to cause observable effects.<sup>19</sup> Impact loading is fundamentally different from impulsive loading. An impact produces: (a) a contact phenomenon in one or both of the colliding objects, such as a scalp contusion or skull fracture; and (b) the transmission and reflection of pressure waves into the system (Fig. 3), for example, the contracoup effect of skull deformation<sup>20</sup> or cavitation.<sup>21–23</sup> If there is no contact phenomenon or wave propagation, the event is not an impact. Slamming a baby or an adult’s head into a pillow is not an impact because there is no wave propagation: the pillow simply gives way, absorbing and diffusing kinetic energy of the moving head such that very little energy must be dissipated by the head and its contents.

The impact of a rigid skull against a nonyielding surface always causes both translational and angular acceleration of the brain unless the force is transmitted exclusively through the center of mass. The relative contributions of the impact-induced translational and angular acceleration components, and their magnitude will determine whether a subsequent injury is primarily focal, primarily diffuse, or a combination of focal and diffuse. The path to the impact (“preimpact impulsive loading”, such as a fall from a moving swing, or a “slam” following a “shake”) is irrelevant and does not contribute to the injury or its characteristics.<sup>24–26</sup>

**Injury parameters and criteria**

Kinematic (motion) parameters such as acceleration (G’s) are usually used to define injury thresholds. It is relatively simple to measure linear acceleration, **a**, in contrast to a quantity such as deformation that can be directly associated with injury. However, kinematic parameters are an incomplete description of the event and may be significantly misleading. Unfortunately, the current federally mandated standards,<sup>27</sup> supplemented by those of private organizations such as the American National Standards Institute<sup>28</sup> and the Snell Foundation,<sup>29</sup> base head injury tolerance on either the peak acceleration, the acceleration-time record, or a function of the acceleration history. The latter, called the HIC (Head Injury Criterion), is defined as

$$HIC = \max_{t_1, t_2, t_2 > t_1} \left[ \frac{1}{t_2 - t_1} \int_{t_1}^{t_2} a dt \right]^{2.5} (t_2 - t_1), \quad (1)$$

where  $t_1$  and  $t_2$  are any 2 points on the acceleration curve. If the HIC is less than 1000, the criterion predicts that there will be no irreversible injury.<sup>30</sup>

These standards specify *linear* acceleration as the tolerance parameter, although *angular* acceleration produces a different and more significant injury pattern.<sup>31,32</sup> Tolerance based on linear acceleration resulted from the pioneering work of Gurdjian.<sup>33,34</sup> His curve, known as the Wayne State



**FIGURE 1.** Impulsive loading (a) Rear loading (b) Front loading.

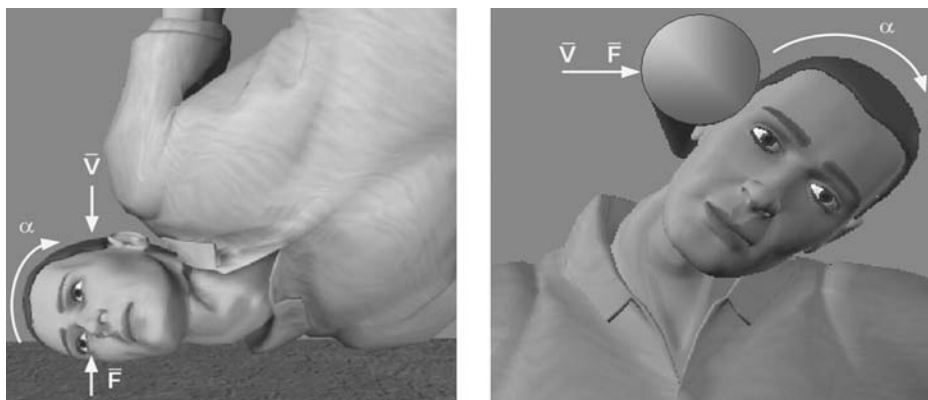


**FIGURE 2.** Impact loading (a) With a fixed object (b) With a moving object.

Tolerance Curve (WSTC), is based on a number of assumptions, including the equivalence of linear skull fracture and the onset of concussion, and the direct extrapolation of the results from cadavers to living humans. The WSTC and others<sup>35</sup> do not differentiate between age, sex, or size, and were expected to apply to infants and children as well as adults. However, this extrapolation is almost certainly invalid because the cerebral mechanical properties and even scaled geometry of infants is quite different from that of adults.<sup>1-7</sup>

Regardless of the utility of the HIC for defining limits of translational acceleration, other criteria have been proposed.<sup>36</sup> A separate criterion is also needed for rotational acceleration and for a combination of rotation and translation occurring simultaneously (as is almost always the case for biologic systems).<sup>37</sup>

Stürtz established *linear* acceleration head tolerance levels for children by reconstructing pedestrian-automobile

impacts.<sup>38,39</sup> He determined that 83g was the limit for the anterior/posterior acceleration when the acceleration lasted more than 3 milliseconds. He also concluded that a peak acceleration of 70g was associated with completely reversible injury, and that 110g was associated with 25% irreversible injury. These limits correspond to HIC values of 350 and 600, respectively, for a 6-year-old child dummy<sup>40</sup>.

The biofidelity and motion of the Child Restraint-Air Bag Interaction (CRABI) anthropometric dummy<sup>41</sup> have been studied by subjecting the dummy to linear and angular acceleration.<sup>42</sup> The author suggested limiting HIC values for the 6-month-old infant of 121 with an acceleration duration of 22 milliseconds (a peak tolerance of 32g), if the values are scaled from adult dummy values of HIC = 1000, an acceleration duration of 15 milliseconds, and a peak acceleration of 85 g. However, the CRABI dummy may not provide adequate biofidelity at impact levels producing significant injury.<sup>42</sup> Experiments using other surrogates were somewhat inconclusive, but indicated no significant difference in tolerance levels between children and adults,<sup>43,44</sup> with values in the range of those found by Stürtz.<sup>39</sup>

Gennarelli and Thibault established *angular* acceleration tolerances by subjecting baboons to severe rotational acceleration replicating automotive impacts.<sup>13,17,32</sup> These experiments were designed to isolate the rotational component of brain acceleration caused by an impact, not to study “whiplash”. The measured angular acceleration corresponding to the observed injuries, from concussion to SDH to DAI, were extrapolated to humans using scaling relations discussed below. These extrapolations were also used for the first of only 3 published scientific experiments conducted to measure the acceleration levels produced by shaking and by impact, and to predict the likely outcome in an infant.<sup>45</sup> The results (Fig. 4) plot angular acceleration as a function of the change in angular velocity, with injury thresholds scaled from primate experiments to a 500 g brain mass. Mean peak tangential accelerations for “shaking” were 9.3 g, while those for “impact” were 428 g, 46 times greater. These impulsive

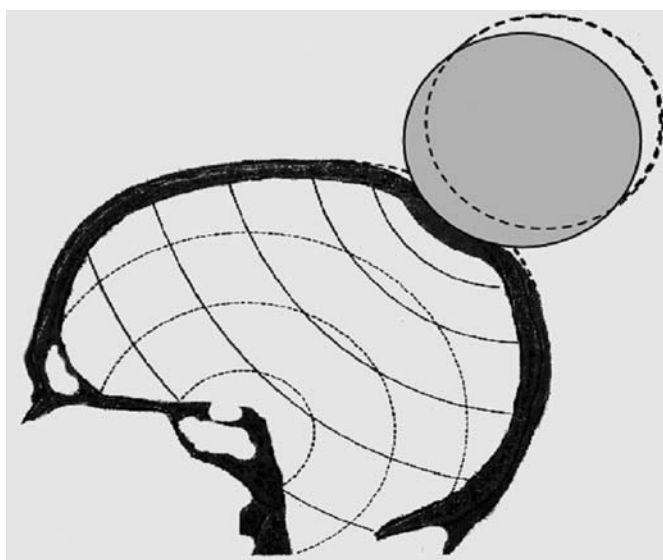


**FIGURE 3.** Contact phenomenon and wave propagation in impact to the head.

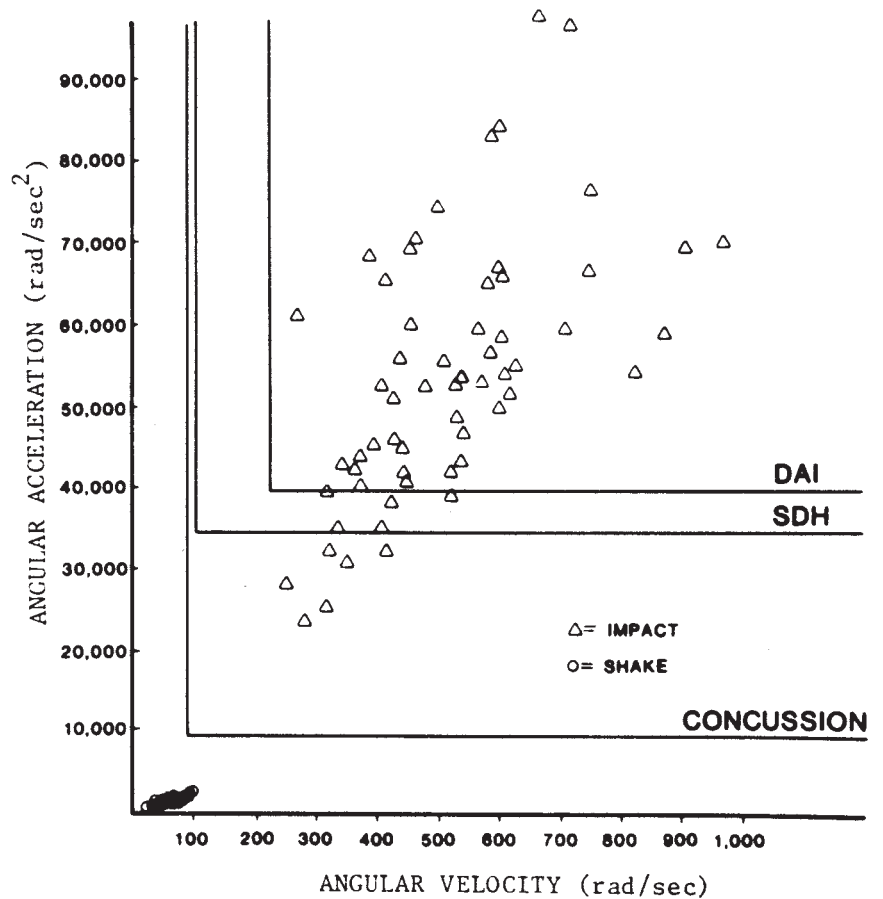


**FIGURE 4.** Angular acceleration as a function of angular velocity scaled to a 500 g brain mass, showing thresholds of concussion, SDH and DAI for both shaking and impact.<sup>44</sup> (Reproduced with permission from Duhaime A-C, Gennarelli TA, Thibault LE, et al. The shaken baby syndrome: a clinical, pathologic and biomechanical study. *J Neurosurg.* 1987;66:409–415.)

loading and impact experiments were repeated with an infant dummy that had a deformable skull.<sup>46,47</sup> In these studies, the ratio of peak impact acceleration to impulsive loading acceleration was reduced from 46 to 39, as expected with a deformable skull model.

The low load level from shaking was substantiated by experiments in our Berkeley laboratory using an anthropometric dummy shaken by a variety of individuals. “Shaking” produced frequencies from 3–5 Hz, with associated total displacements from 102–152 mm (4–6 in). If the excursion and frequency are modeled as “simple harmonic motion”,<sup>48</sup> a repetitive movement at a uniform rate from an equilibrium position with an amplitude, A, half (51–76 mm [2–3 in]) of the total displacement, the motion approximates an actual “shaking”. Using this model, the maximum linear acceleration,  $a_{max} = A\omega^2$ , where  $\omega$  is the angular velocity, was 7.7 g, slightly less than that found in the previous tests.<sup>45–47</sup> When the actual digital camera data rather than the model were analyzed, the result was 15 g, higher than the model because the real-time motion is not that of a rigid-body.

Two sets of whiplash tests on anesthetized baboons,<sup>31,49</sup> modeling a rear-end vehicular collision, caused acute SDH and spinal cord injuries with angular velocities

above 500 rad/s and angular accelerations of more than 10 krad/s<sup>2</sup>. (10 krad/s<sup>2</sup> is 10,000 ft/s<sup>2</sup>, or 155 g’s, at a radius of 1 foot.) These values are typical of head accelerations under vehicular impact conditions. The results of these experiments have been cited incorrectly<sup>50–52</sup> to support the mechanism for Shaken Baby Syndrome (SBS), the authors apparently not understanding that the results replicated the effects of a 48.3 km/h (30 mph) vehicular impact, not a 9.3 g “shake”.

**Scaling and impulsive loading**

Different sized brains do not have the same injury thresholds. However, it is possible to convert or scale brain injury thresholds associated with impulsive loading from many animals to humans. These species relationships are based on an empirically verified equation, derived from theory, where the ratio of the accelerations is equal to the inverse of the brain mass ratio raised to the 1/3 power for linear acceleration and the 2/3 power for angular acceleration (Fig. 5).<sup>53,54</sup> Scaling assumes complete material property, structural, and geometric similarity between the various systems compared. The head of an infant is smaller and geometrically unlike that of an adult.<sup>55–57</sup> The structural properties of the infant skull (ease of deformation and decreased threshold

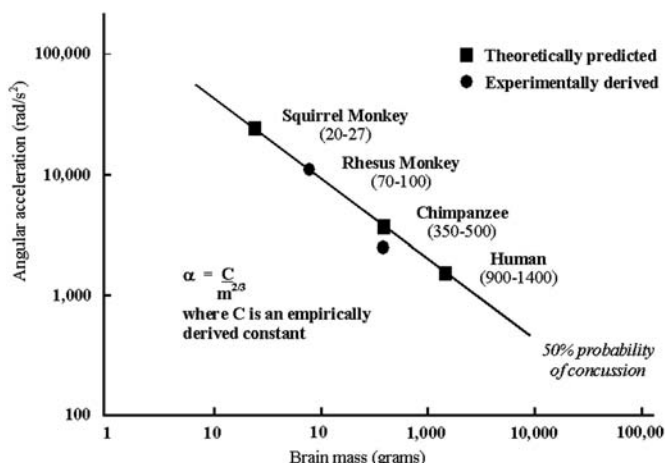


**FIGURE 5.** Concussion tolerance as a function of angular acceleration and brain mass.<sup>52</sup> (Modified and reproduced with permission from Ommaya AK, Yarnell P, Hirsch AE, et al. Scaling of experimental data for cerebral concussion in subhuman primates to concussive threshold for man. In: *Proc 11<sup>th</sup> Stapp Car Crash Conf* New York: SAE; 1967: 47–52. SAE Paper 670906.)

to fracture), and the mechanical properties of the infant brain are also different from those of an older child or adult.<sup>5,46,58,59</sup> These actual and potential differences between adult and infant brain structural and mechanical properties mean that impact-induced acceleration tolerances for nonhuman adult primates should not be scaled to human infants.

**Deformation and failure characteristics of objects**

A SDH is usually caused by rupture of the parasagittal bridging veins. The mechanical and failure behavior of these vessels have been determined by load tests that provide either force-deformation or stress-strain relations up to rupture. Unidirectional stress is force per unit area,  $\sigma = F/A$ , while deformation (strain) may be through extension, compression, or “shear”. Mathematically, uniaxial strain  $\epsilon = (\Delta L/L_0)$  where  $\Delta L$  is the change in length and  $L_0$  is the original length.<sup>8,48</sup>

The behavior of all solid materials under loading conditions is characterized either by a relationship between stress and strain (and possibly time), a constitutive equation, or by a load-deformation curve, a structural designation. Solid material behavior is characterized as elastic, or time-independent and reversible, when a substance subjected to a force immediately returns to its original shape upon unloading along the same path as the loading curve. The behavior is viscoelastic when internal energy dissipation significantly delays the return of the deformation to its original state upon unloading and/or the unloading path is significantly below the loading curve. It is plastic when a substance (such as clay)

retains a permanent deformation after load removal. Most biologic tissues, including brain, are viscoelastic and their behavior depends on the rate of load application. Only teeth, nails, and adult bone have nearly elastic behavior before failure.

The critical load is that where mechanical (structural) failure is produced, although physiological (functional) disruption may occur at lower levels. The critical value is the ultimate strain,  $\epsilon_u$ , corresponding to an ultimate stress,  $\sigma_u$ , where there is total mechanical disruption (fracture of the skull or rupture of the bridging veins). The likelihood of bridging vein rupture also depends on the orientation of the vessels to the superior sagittal sinus. Veins anterior to the midfrontal pole drain posteriorly to join the sinus in the same direction as its flow, and are subject to maximum extension strain only with a frontal impact. Vessels at the midfrontal pole enter the sinus perpendicular to it. Veins posterior to the midfrontal pole drain anteriorly into the sinus, in the direction apposite its flow, and experience maximum extension strain with an occipital impact.<sup>10,11,60,61</sup>

An example of a set of nonlinearly elastic relationships of vessels under slow loading conditions is shown in Figure 6.<sup>62,63</sup>

**Differences in adult and infant skull properties and the response to impact and impulsive loads**

The mechanical characteristics of the infant and adult skull are not the same. The adult skull is only slightly deformable prior to fracture. The infant skull is not rigid, and should be considered as a segmented unit of loosely associated curved plates with interspersed soft membranes (sutures and fontanelles).<sup>55,64</sup>

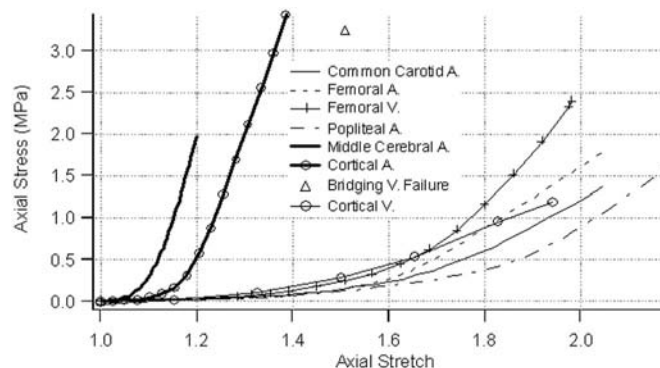


**FIGURE 6.** Quasi-static stress versus stretch behavior for various fresh cortical arteries and veins.<sup>59</sup> (Reproduced with permission from Monson KL, Goldsmith W, Barbaro N, et al. Static and dynamic mechanical and failure properties of human cerebral blood vessels. In: *Crashworthiness, Occupant Protection and Biomechanics in Transportation Systems*. New York, ASME; 2000. AMD 246/BED 49:255–65.)

Thibault and Margulies<sup>5,6,65,66</sup> compared the mechanical properties of the skulls of human infants and adults to those of infant and adult pigs. They found significant variation in the failure stress of the skull of the neonate, the young child, and the adult, with an increase in stress to fracture of more than a factor of 10 from the newborn to the adult (Fig. 7). The variation in the elastic modulus, E, showed a 10-fold increase (Fig. 8), supporting nearly identical conclusions from earlier tests.<sup>40,67,68</sup>

The Consumer Products Safety Commission (CPSC)<sup>56</sup> has published a compendium on the geometric properties of the infant head. An earlier work indicated substantial difference in the vasculature of infants and adults.<sup>57</sup> The neonates had thinner and fewer vessels than the mature cortex,<sup>69</sup> the blood/brain barrier was incompletely developed, and the infant blood cerebral blood flow and oxygen consumption were more than twice that in adults.

These structural differences cause the injury mechanism for an infant to be fundamentally different from that of an older child or adult. Impact loading of the compliant infant skull/brain unit produces potentially damaging levels of strain within the entire structure. Deformation, not impact-induced angular acceleration, is the critical factor. Nonimpact loading (“shaking”) may result in strains of the neurovascular structures, but there is no associated skull deformation. Biomechanical studies have demonstrated that the head accelerations generated by shaking are below the thresholds for

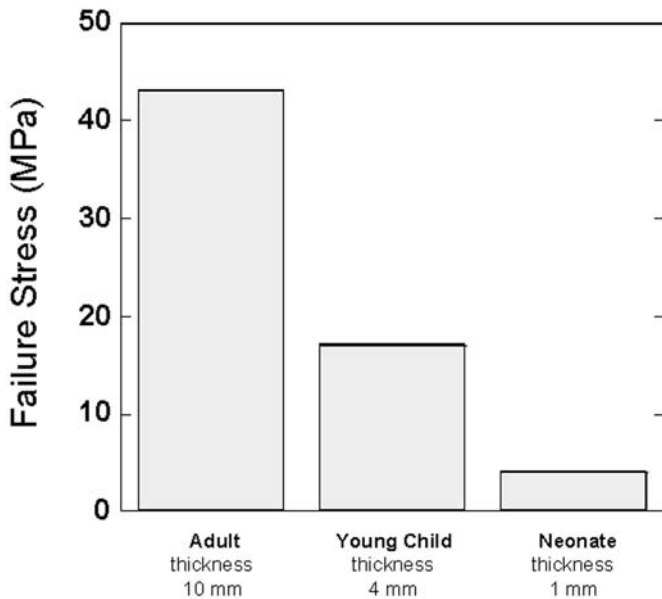


FIGURE 7. Skull failure stress for the neonate, young child and adult.<sup>8</sup> (Reproduced with permission from Ommaya AK, Goldsmith W, Thibault L. Biomechanics and neuropathology of adult and pediatric head injury. *Br J Neurosurg.* 2002;16: 220–242.)

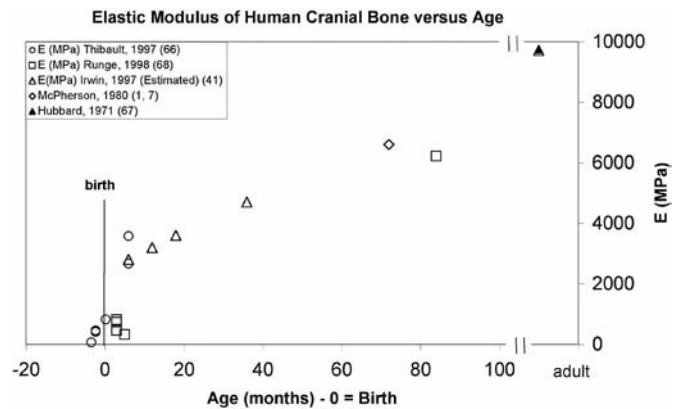


FIGURE 8. Elastic modulus of human cranial bone versus age. (Created by Kirk L. Thibault, PhD, from data in the studies referenced.)

traumatic DAI, SDH, and even concussion. If one could “shake” an infant or a child, or an adult for that matter, vigorously enough to cause traumatic DAI or SDH, there will be significant structural neck damage, including the cranio-cervical junction (F.A. Bandak, personal communication).<sup>70–71</sup> Shaking simply does not generate accelerations that exceed any known injury tolerance values for traumatic brain injury.

The material and structural properties of the skull and brain are age-dependant. The transition from the predominately deformation-mediated impact response in an infant to a predominately acceleration (impulsive)-mediated response in an older child or adult is a continuum. It is not possible, with today’s data, to state a specific age at which the final change occurs. In vivo and surrogate biomechanical experiments to further define the parameters of age-dependency must be assisted by various imaging technologies including MRI, a careful neurologic examination for signs of cervical spinal cord or brain stem injury in a child who is living, and a complete and careful postmortem examination including posterior neck dissection if death occurs.

**Analysis of impacts due to falls**

The linear impulse-momentum relation derived from Newton’s Second law applied over time can be used to analyze an impact caused by a fall. The relationship states that the area under the force-time (F-t) curve is equal to the change of linear momentum; in practice, the product of mass, m, times the change of velocity,  $\Delta v$ .<sup>19,48</sup> For contact events, the maximum force generated can be closely approximated by the expression  $F_{max} = 2m\Delta v/\tau$ , where  $\tau$  is the duration of contact.<sup>72</sup> If a 0.91 m (3 ft) tall child falls by backward rotation about the soles of his/her feet, the translational impact velocity is 4.24 m/s (13.9 ft/s) at the occiput, and the angular impact velocity is 4.63 rad/s. Our Berkeley laboratory

determined that contact duration  $\tau$  is 3–7 milliseconds by dropping a weight-adjusted cadaver skull onto the edge of a hardwood stair step. If only the impact of the head produces the contact force (the weight of the body does not contribute), the contact time is taken as 5 milliseconds and the head weighs 22.4 Newtons (N) (5.3 lb), 20% of the body weight of 112 N (26.4 lb), the peak force is 4070 N (915 lb) from the linear impulse-momentum relation, assuming a triangular force profile. This is a peak acceleration of 173 g, nearly sixteen times greater than would be obtained by shaking and twice as great as the tolerance limit suggested by Stürtz.<sup>39</sup> These linear acceleration values approach those obtained from the previously described actual experiments;<sup>45–47</sup> the small differences are most likely due to variation in surface characteristics or a conservative assumption for the contact time in the above analysis.

There has been sworn testimony in courts of law by expert witnesses who state that trauma caused by shaking is equivalent to a fall from a two-story (or higher) window onto the pavement.<sup>73</sup> If such a fall is head first with the body in a vertical or near vertical position at impact, the forces on the head can be calculated from the linear impulse-momentum law. Assuming that the weight of the child is 66.7 N (15 lb), that the fall height is 5.63 m (18 ft), and that the contact duration is a very conservative 10 milliseconds, the impact velocity will be 10.37 m/s (34 ft/s), and the peak contact force 14,190 N (3167 lb). This exceeds by at least an order of magnitude the force that can be exerted by shaking, and at least 3 times that considered from the data of Gurdjian<sup>30</sup> as the human tolerance limit. The analogy of “shaking” injury to that from a two-story fall is not justifiable.

It has also been stated that falls from low heights do not produce significant injury or death.<sup>74–76</sup> However, Mohan et al<sup>77</sup> analyzed 30 falls in children under the age of 10, and reconstructed 6 of them using the MVMA Two-Dimensional Crash Victim Simulator computer model. The authors concluded that falls as low as 2 meters may cause serious injury or death.

Plunkett documented 18 fatal falls from heights of 0.6 to 3 m (2–10 ft).<sup>24</sup> One of these falls was coincidentally videotaped, permitting an approximate analysis of the contact loads. A 23-month-old girl who weighed 129 N (29 lb) and was 0.838 m (33 in) tall fell from a play structure onto a 10 mm (0.39 in) thick carpet without foam backing covering a concrete floor. She had lost her grip on a rail when she was in a nearly horizontal position approximately 1.07 m (42 in) above the ground. She struck the ground first with her outstretched hands and then with her right upper frontal forehead, followed by her right shoulder (Fig. 9). Although alert immediately after the fall, she became unconscious within approximately 5 minutes. She was taken to a tertiary care hospital where a 100 mL right-sided SDH was immediately evacuated. The attending medical staff documented

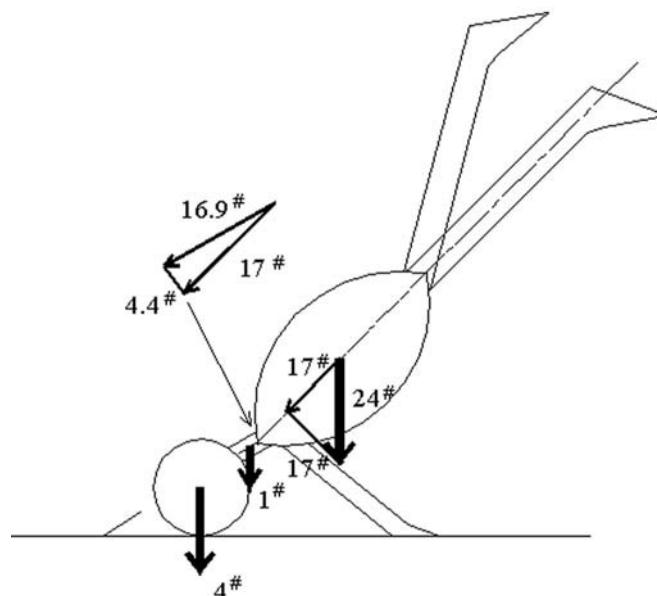


FIGURE 9. Idealized contact position and loads in the fall of a 29 lb (12.9K) child from a height of 42 in (1.07 m).

extensive bilateral retinal hemorrhage (RH) following the surgery. Postoperatively, she developed refractory cerebral edema and was removed from life support after 1.5 days. An autopsy showed a small residual right SDH, cerebral edema with herniation, and a 40 × 45 mm (1.58 × 1.77 in) right frontal scalp contusion. There was no skull fracture.

Her unsupported weight caused rotation about her feet until her body was at an angle of approximately 45° from the horizontal, with her head and neck inclined at approximately 30° to the horizontal. Her feet then disengaged the play structure and she fell freely with her center of gravity dropping 0.483 m (19 in) until she struck the carpet. If the moment of inertia (the property of an object to resist rotation) taken at the center of mass, G, is idealized as a uniform cylinder with a radius of 101.6 mm (4 in), her moment of inertia about her feet is 3.116 N-m-s<sup>2</sup> (27.57 lb-in-s<sup>2</sup>).<sup>48</sup> The impact velocity due to rotation, using a number of simplifying assumptions, is 4.36 m/s (14.3 ft/s) whose vertical component is 3.78 m/s (12.4 ft/s). The concurrent velocity due to the vertical motion of the center of gravity in the fall is 3.05 m/s (10 ft/s), so that the impact velocity of the head is 6.83 m/s (22.4 ft/s) (compared with 4.57 m/s [15 ft/s] if the body remained entirely horizontal). This calculation ignores the braking effect of the outstretched arms, so that the likely impact speed of the head was of the order of 4.57–6.10 m/s (15–20 ft/s).

Since the skull, scalp and carpet were not available to measure compliance, the contact duration will be conservatively assumed to be 10 milliseconds. The child’s weight distribution will be assumed to be 107 N (24 lb) for torso,

legs and arms, 4.45 N (1 lb) for the neck and 17.8 N (4 lb) for the head. The 107 N (24 lb) component will be resolved along and perpendicular to the spine (the centerline of the body); this component, further resolved, is transmitted along the neck to the head, and the full weight of the head contributes to the impact event. This results in an equivalent vertical force at the contact point due to the weight components of 60 N (13.5 lb). The peak impact contact force  $F_m$  is calculated from the adjusted linear impulse-momentum equation, using both the equivalent weight of 60N (13.5 lb) and the full child's weight of 129 N (29 lb). The clockwise movement of her head is small and will be ignored. The peak forces and corresponding maximum compressive stresses, assuming that contact occurred over the entire area of the contusion, are (Table 1).

This child did not have a skull fracture (consistent with a well-distributed impact load against a flat surface), and the area of her scalp contusion was less than 2.25 in<sup>2</sup>. Her skull failure stress was approximately 16–20 MPa (Fig. 7). Her maximum skull stress computed for a duration of 10 milliseconds is less than 16–20 MPa for both sets of conditions used in the calculations. Although the peak compressive stress is not directly related to the tensile failure limit of the parasagittal bridging veins, this limit of 3.5 MPa<sup>11</sup> is of the same order of magnitude.

Finite element modeling (FEM) of heads subjected to various types of impact and impulsive loading supports this type of analysis.<sup>68,78</sup> However, until validated by appropriate experiments, the FEM results must be interpreted cautiously.

**Recent studies**

Geddes et al did the first rigorous analysis of the infant brainstem in presumed nonaccidental head injury.<sup>79</sup> They identified specific neuropathological findings in head injury for 53 infants and children, and found statistically significant patterns of age-related injury. The group of 37 infants 20 days to 9-months-old tended to have injuries limited to the head, including skull fracture (43%). Twenty-six of the 37 (70%) had SDH. The SDH was a “thin-film” in 21 of the 26 (84%). Eleven (30%) of the 37 infants had immunohistochemical

evidence for axonal damage at the craniocervical junction. Only 2 infants had traumatic diffuse axonal injury (DAI). Children thirteen months or older tended to have larger SDH, and if there was traumatic axonal damage, the injury patterns were similar to those reported in adults. The authors concluded that traumatic DAI is uncommon in children thought to have inflicted head injury.

In a second study, these authors compared the neuro-pathological findings in the younger group of 37 infants to a control group of 14 similarly aged infants who died of other causes.<sup>80</sup> The most common finding in the study group was global hypoxic damage (84%). Two cases had traumatic axonal injury, and both had severe contact head injuries with skull fractures. Epidural cervical hemorrhage, and focal axonal brainstem and cervical nerve root damage, was found in 11 cases, with none in the control group, suggesting relative vulnerability at the infant craniocervical junction. The authors concluded that the lack of widespread severe axonal damage in the infant could be explained in one of 2 ways: either the nonmyelinated axons of the immature brain are less susceptible to damage during traumatic loading, or in “shaking type injuries” the brain is not exposed to the forces necessary to cause traumatic DAI. Because of the trivial nature of the brain stem pathology in a few of the cases, coupled with a lack of damage to soft tissues in the neck, the authors suggested that hyperextension/hyperflexion at low loading levels, below those necessary to cause diffuse brain damage, may injure nerve fibers at the craniocervical junction. The resulting apnea leads to severe hypoxia and cerebral edema, and the immediate signs and symptoms may mimic those previously thought due exclusively to parasagittal vessel failure caused by violent head rotation.

Margulies and Thibault’s study emphasized the critical role of skull deformation in infant impact head injury<sup>6</sup> by measuring infant skull and suture properties, and modeling differences between infants and adults with regard to the consequences of impact loading. They first confirmed that infant pig and infant human skull and suture properties were comparable, then measured infant pig cranial bone and suture failure using tensile and three-point bending. They found that the elastic modulus, ultimate stress, and energy absorbed to failure increases, and ultimate strain decreases, with age for both skulls and sutures. The authors then constructed 2 finite element models of a one-month-old infant head, using the above-determined infant values for one and adult values for the other. When the models were impact loaded, the skull and brain of the infant model underwent larger cranial shape changes and had a more diffuse pattern of brain distortion than the adult model. Dynamic herniation of the brainstem through the foramen magnum as a result of these shape-change induced deformations during impact, or quasi-static herniation of the brainstem during secondary brain swelling,

**TABLE 1.** Impact Force and Stress

Weight		Impact velocity		Peak force		Peak compressive stress	
N	lb	m/s	ft/s	kN	lb	MPa	psi
60	13.5	4.57	15	5.59	1258	3.1	449
60	13.5	6.10	20	7.46	1677	4.13	599
129	29.0	4.57	15	12.02	2702	6.65	965
129	29.0	6.10	20	16.02	3602	8.88	1287

may cause focal traumatic axonal injury mimicking “shaking”/hyperextension.

## Abuse

Either abuse or an accident may cause head injury in an infant or child.<sup>81,82</sup> However, it is not possible to differentiate a deliberate impact from an accidental fall under the same mechanical circumstances (speeds, surfaces, configurations) by biomechanical analysis since the mechanism and injury patterns will be identical.

There are other “hallmarks” of “nonaccidental” infant head trauma that need to be critically evaluated. For example, Greenwald<sup>83</sup> and the American Academy of Ophthalmology<sup>84</sup> have stated that retinal hemorrhage (RH) with particular characteristics is “proof” of shaking. Greenwald and others<sup>52,83,85</sup> state that the mechanism for RH in SBS is impulsive loading, with vitreous traction splitting the retina. However, *external* rotation of the eye as would occur with “shaking” (with a moment of inertia about C4-5) is curvilinear not rotational. For *internal* rotation (the eye rotating about its own center of mass) to cause traumatic injury, scaling suggests that the level of acceleration would need to be greater than  $100,000r/s^2$ , or 6250g at a radius of 3/8 in. Experimental data indicate that the actual mechanism for RH is functional or mechanical venous occlusion.<sup>86–89</sup> RH of all types and distributions has been documented in ruptured vascular malformations,<sup>90</sup> increased intrathoracic pressure,<sup>91</sup> bungee jumping,<sup>92,93</sup> atypical lymphohistiocytic proliferations,<sup>94</sup> short falls,<sup>24</sup> anemia,<sup>95</sup> and severe contact head injury.<sup>96,97</sup> The question is not whether shaking causes RH, but under what mechanical constraints (rate, etc.) does cerebral edema or other causes of venous occlusion result in RH?

Does new bleeding/“rebleeding” in an established SDH require proximate trauma? This question can be approached biomechanically, but there is little definitive information concerning the sequence of events. For example, the rate of efflux from various types of tears in cerebral vessels has not been quantified, nor has the rate of resorption of blood in the subdural or subarachnoid spaces been determined. The “natural history” of an acute SDH includes new bleeding without proximate trauma, and has been documented in a series of patients with acute SDH followed by computed tomography scanning.<sup>98</sup>

All of the above and preceding questions *demand* an interdisciplinary effort involving physicians, biomechanicians, and other specialists to determine the actual unique, age-dependant mechanisms of pediatric head injury. The effort should be directed toward constructing a dummy with realistic head and neck characteristics and subjecting this device to controlled loading. The experiments should be paralleled by analytical and numerical studies of the physical events and extended to the cellular level.<sup>99–106</sup> When accept-

able correlation of predictions and tests is achieved, a major step will have been taken to resolve these issues.

## CONCLUSIONS

1. It is usually not possible, based on the *medical* signs and symptoms, to determine if a given head injury is due to an accident or abuse. Therefore, it is critical that health care professionals who are asked to make this determination understand injury *mechanisms*, tolerance thresholds, and the limitations of a mechanistic approach.

2. Tolerance thresholds for infants, and especially those less than 3-months-old, should not be scaled from adult acceleration or deformation data.

3. The known mechanical properties of the infant *skull* permit construction of a biofidelic dummy that can be subjected to a variety of loading conditions. The results can be compared with established or future injury criteria, providing a distinctive database for assessing the *mechanical* cause of an injury. The results of such experiments can be correlated with data from analytical modeling and/or primate experiments.

4. It is not currently possible to construct a biofidelic infant *neck* because the mechanical properties of the infant neck are not known.

5. There is an urgent need for close collaboration between physicians and biomechanicians to objectively and scientifically evaluate infant head injury, and to assist in determining the mechanical basis, diagnosis and treatment of infant head trauma.

## ACKNOWLEDGMENTS

The authors express sincere appreciation to Drs. Kirk Thibault, Kenneth Monson, and Andrea Goldsmith for major assistance in the composition of this article.

## REFERENCES

- McPherson GK, Kriewall TJ. The elastic modulus of fetal cranial bone: a first step towards an understanding of the biomechanics of fetal head modeling. *J Biom.* 1980;13:9–16.
- Kriewall TJ, McPherson GK, Tsai A Ch. Bending properties and ash content of fetal cranial bone. *J Biom.* 1981;14:73–79.
- Kriewall TJ. Structural, mechanical and material properties of fetal cranial bone. *Am J Obstet Gynec.* 1982;143:707–714.
- Kriewall TJ, Akkas N, Bylski DI, et al. Mechanical behavior of fetal dura mater under large axisymmetric inflation. *J Biom Eng.* 1983;105:71–76.
- Thibault KL, Margulies SS. Age-dependent material properties of the porcine cerebrum: effect on pediatric head injury criteria. *J Biom.* 1998;31:1119–1126.
- Margulies SS, Thibault KL. Infant skull and suture properties: measurements and implications for mechanisms of pediatric brain injury. *J Biom Eng.* 2000;122:364–371.
- McPherson GK, Kriewall TJ. Fetal head modeling: an investigation utilizing a finite element model of the fetal parietal bone. *J Biom.* 1980;13:17–26.
- Ommaya AK, Goldsmith W, Thibault LE. Biomechanics and neuropathology of adult and paediatric head injury. *Br J Neurosurg.* 2002;16:220–242.

9. Goldsmith W. The state of head injury biomechanics – past, present and future. Part I. *Crit Rev Biomed Engng*. 2001;29:441–600.
10. Löwenhielm P. Dynamic properties of parasagittal bridging veins. *Z Rechtsmed*. 1974;74:55–62.
11. Lee MH, Haut RC. Insensitivity and tensile breakdown properties of the human parasagittal bridging veins to strain rate dependence in biomechanics of subdural hematoma. *J Biom*. 1989;22:532–542.
12. Ommaya AK, Thibault LE, Bandak F. Mechanisms of head injury. *Int J Impact Eng*. 1994;15:525–560.
13. Ommaya AK, Corrao P, Letcher PS. Head injury in the chimpanzee: biodynamics of traumatic unconsciousness. *J Neurosurg*. 1963;39:152–166.
14. Prange MT, Margulies SS. Regional, directional and age-dependent properties of the brain using physical models to determine cortical strains in the head during dynamic loading. In: *Proc Ann Intern Conf IEEE Engng in Med and Bio Soc*. New York: IEEE. 1989;3:816–817.
15. Arbogast KB, Margulies SS. Regional differences in mechanical properties of the porcine central nervous system. In: *Proc 42<sup>nd</sup> Stapp Car Crash Conf 1997*. Warrendale, PA: Society of Automotive Engineers. SAE Paper 973336:293–300.
16. Kleiven S. Influence of impact direction on the human head in prediction of subdural hematoma. *J Neurotr*. 2003;20:365–379.
17. Gennarelli TA, Thibault LE, Adams JH, et al. Diffuse axonal injury and traumatic coma in the primate. *Ann Neurol*. 1982;12:264–274.
18. Smith SL, Andrus PK, Gleason DD, et al. Infant rat model of the shaken baby syndrome: preliminary characterization and evidence for the role of free radicals in cortical hemorrhaging and progressive neuronal degeneration. *J Neurotr*. 1998;15:693–705.
19. Goldsmith W. *Impact: The Physical Theory and Behaviour of Colliding Solids*. London: Edward Arnold Ltd.; 1960. Mineola, NY: Dover Publications; 2001.
20. Ommaya AK, Grubb RL, Naumann RA. Coup and contre-coup injury: Observations on the mechanics of visible brain injuries in the Rhesus Monkey. *J Neurosurg*. 1971;35:503–516.
21. Gross AG. Impact thresholds and brain concussion. *Aviation Med*. 1958;29:725–732.
22. Lubock P, Goldsmith W. Experimental cavitation studies in a model head-neck system. *J Biom*. 1980;13:1041–1052.
23. Nusholtz GS, Glascoe LG, Wylie EB. Cavitation during head impact. In: *Occupant Protection and Injury Assessment in the Automotive Crash Environment, SP 1231*. Warrendale, PA: Society of Automotive Engineers; 1997:151:–623.
24. Plunkett J. Fatal pediatric head injuries caused by short distance falls. *Am J Forens Med Pathol*. 2001;22:1–12.
25. Goldsmith W. Fatal pediatric head injuries caused by short distance falls (letter). *Am J Forens Med Pathol* 2001;22:334–336.
26. Plunkett J. Fatal pediatric head injuries caused by short distance falls (letter). *Am J Forens Med Pathol* 2002;23:103–105.
27. Hess RL, Weber K, Melvin JW. A review of research on head impact tolerance and injury criteria related to occupant protection. In: *Head and Neck Injury Criteria: A Consensus Workshop*. Washington, DC: U S Government Printing Office; 1983. (DOT HS 806 434):183–194.
28. American National Standards Institute. *American National Standard for Protective Headgear – for Bicyclists*. Washington, DC: American National Standards Institute; April 1984. ANSI Z90.
29. Snell Memorial Foundation. *Standards for Protective Headgear for Use With Bicycles. Child Helmet. Addendum for CPS Requirements*. North Highlands, CA: Snell Memorial Foundation; 1995.
30. Goldsmith W. Meaningful concepts of head injury. In: *Proc 1989 International Research Council on the Biomechanics of Impact Conf*. Bron, France: IRCOBI. 1989;1:–12.
31. Ommaya AK, Hirsch AE. Tolerances for cerebral concussion from head impact and whiplash in primates. *J Biom*. 1971;4:13–21.
32. Gennarelli TA, Thibault LE. Biomechanics of acute subdural hematoma. *J Trauma*. 1982;22:680–686.
33. Gurdjian ES, Lissner HR, Patrick LM. Protection of the head and neck in sports. *JAMA*. 1962;182:509–512.
34. Gurdjian ES. *Impact Head Injury: Mechanistic, Clinical, and Preventive Correlations*. Springfield, IL: CC Thomas; 1975.
35. Ono K, Kikushi A, Nakamura M, et al. Human head tolerance in sagittal impact reliable estimation deduced from experimental head injury using subhuman primates and human cadaver skulls. In: *Proc 24<sup>th</sup> Stapp Car Crash Conf*. Warrendale, PA: Society of Automotive Engineers; 1980:101:–160. SAE Paper 801303.
36. Sturgess CE. A thermomechanical theory of impact trauma. In: *Proc ImechE J Automobile Div*. London: Institution of Mechanical Engineers; 2003: In press.
37. Newman JA. A generalized model for brain injury threshold. In: *Proc 1986 International Research Council on the Biomechanics of Impact Conf*. Bron, France: IRCOBI; 1986: 121:–131.
38. Stürtz G. Correlation of dummy-loadings with real injuries of children by repetition tests. In: *Proc V<sup>th</sup> International IRCOBI Conf*. Bron, France: IRCOBI; 1980:194:–208.
39. Stürtz G. Biomechanical data of children. In: *Proc 24<sup>th</sup> Stapp Car Crash Conf*. Warrendale, PA: Society of Automotive Engineers; 1980. (SAE Paper 801313):525–59.
40. Melvin JW. Injury assessment reference values for the CRABI-6 month infant dummy in a rear-facing infant restraint with airbag deployment. *SAE J for Passenger Cars*. Warrendale, PA: Society of Automotive Engineers; 1995. SAE Paper 950872:1553–64.
41. Irwin A, Mertz HJ. Biomechanical basis for the CRABI and Hybrid III child dummies. In: *Proc 41<sup>st</sup> Stapp Car Crash Conf*. Warrendale, PA: Society of Automotive Engineers; 1995. (SAE Paper 973317):261–72.
42. Klinich KD, Hulbert GM, Schneider LW. Estimating infant head injury criteria and impact response using crash reconstruction and finite element modeling. *Stapp Car Crash J*. 2002;46: Paper O2S-32.
43. Lucchini E, Weissner R. Difference between the kinematics and loadings of impacted adults and children: Results from dummy tests. In: *Proc 1980 International Research Council on the Biomechanics of Impact Conf*. Bron, France: IRCOBI; 1980:165:–78.
44. Stecherbatcheff G, Tarrière C, Duclos P, et al. Simulation of collisions between pedestrians and vehicles using adult and child dummies. In: *Proc 19<sup>th</sup> Stapp Car Crash Conf*. Warrendale, PA: Society of Automotive Engineers; 1975. (SAE Paper 751167):147–53.
45. Duhaime A-C, Gennarelli TA, Thibault LE, et al. The shaken baby syndrome: a clinical, pathological and biomechanical study. *J Neurosurg*. 1987;66:409–415.
46. Prange MT, Coats B, Raghupathi R, et al. Rotational loads during inflicted and accidental infant head injury. *J Neurotr* 2001;Abst.D8;18: 1142.
47. Prange MT, Coats B, Duhaime A-C, et al. Anthropomorphic simulations of falls, shakes, and inflicted impacts in infants. *J Neurosurg*. 2003;99:143–150.
48. Berger SA, Goldsmith W, Lewis ER, eds. *Introduction to Bioengineering*. Oxford: Oxford University Press; 1996, 2000.
49. Ommaya AK. Trauma to the nervous system. *Ann Roy Coll Surg Engl*. 1966;39:317–347.
50. Caffey J. The whiplash shaken infant syndrome: manual shaking by the extremities with whiplash-induced intracranial and intraocular bleedings, linked with residual permanent brain damage and mental retardation. *Pediatrics*. 1974;54:396–403.
51. Guthkelch AN. Infantile subdural hematoma and its relationship to whiplash injuries. *Brit Med J*. 1971;2:430–431.
52. Lonergan GJ, Baker AM, Morey MK, et al. Child abuse: Radiologic-pathologic correlation. *Radiographics*. 2003;23:811–845.
53. Ommaya AK, Yarnell P, Hirsch AE, et al. Scaling of experimental data for cerebral concussion in sub-human primates to concussive threshold for man. In: *Proc. 11<sup>th</sup> Stapp Car Crash Conf*. New York: Society of Automotive Engineers; 1967. (SAE Paper 670906):47–52.
54. Ljung C. On scaling in head injury research. In: *Proc V<sup>th</sup> Intern IRCOBI Conf on the Biomechanics of Impacts*. Bron, France: IRCOBI; Sept. 9–11, 1980; 209–217.
55. Netter FH. *Atlas of Human Anatomy*. Summit, NJ: Ciba-Geigy Corp; 1989.
56. Schneider LW, Lehman RJ, Flug M, et al. *Size and Shape of the Head From Birth to Four Years. Final Report to the Consumer Products Safety Commission*. Washington, DC: Univ of Michigan Transp Res Inst 1986; UMTRI-86-2.

57. Stehbens WE. *Pathology of the Cerebral Blood Vessels*. St. Louis: Mosby;1972.
58. Thibault KL, Margulies SS. Age-dependant material properties of the porcine cerebrum: Effect on pediatric inertial head injury criteria. *J Biomech*. 1998;31:1119–1126.
59. Prange MT, Margulies SS. Regional, directional, and age-dependant properties of the brain undergoing large deformations. *Trans ASME*. 2002;124:244–252.
60. Oka K, Rhoton AJ, Barry M, et al. Microsurgical anatomy of the superficial veins of the cerebrum. *Neurosurg*. 1985;17:711–748.
61. Huang HM, Lee MC, Chiu WT, et al. Three-dimensional finite element analysis of subdural hematoma. *J Trauma*. 1999;47:538–544.
62. Monson KL, Goldsmith W, Barbaro N, et al. Static and dynamic mechanical and failure properties of human cerebral blood vessels. In: *Crashworthiness, Occupant Protection and Biomechanics in Transportation Systems*. New York: ASME; 2000. AMD 246/BED 49:255–65.
63. Monson KL, Goldsmith W, Barbaro N, et al. Axial mechanical properties of fresh human cerebral blood vessels. *J Biom Engng*. 2003;125:288–294.
64. Sobotta J. *Atlas of Human Anatomy 1927–1928*. Edited from the 6<sup>th</sup> German edition by JP McMurrich, 1 and 3. New York: GE Stechert; 1927–28.
65. Margulies SS, Thibault LE. An analytical model of traumatic diffuse brain injury. *J Biom Eng*. 1989;111:241–249.
66. Thibault KL. *Pediatric Head Injuries: the Influence of Brain and Skull Properties* [dissertation]. Philadelphia: University of Pennsylvania; 1997.
67. Hubbard RP. Flexure of layered cranial bone. *J Biomech*. 1971;4:251–263.
68. Runge CF, Yousses A, Thibault KL. Material properties of human infant skull and suture: experiments and numerical analysis. In: *Injury Prevention Through Biomechanics Symposium, National Center for Injury Prevention and Control*. Detroit: Centers for Disease Control; 1998. Report 1–1998.
69. McMinn RMH, Hutchings RT, eds. *Color Atlas of Human Anatomy*. Chicago: Year Book Med Publ, Inc.; 1977.
70. Duncan M. Laboratory note: On the tensile strength of the fresh adult fetus. *BMJ* 1874;2:763–764.
71. Mertz HJ, Patrick LM. Strength and response of the human neck. In: *Proc of the 15<sup>th</sup> Stapp Car Crash Conference*. Warrendale, PA: Society of Automotive Engineers; 1971. SAE Paper 710855:2903–28.
72. Goldsmith W, Kabo JM. Performance of baseball caps. *Am J Sports Med*. 1982;10:31–37.
73. 2001 WL 1630083 (Colo. App.). Colorado Court of Appeals, Div. 1. No. 00CA0312.
74. Chadwick DL, Chin S, Salerno C, et al. Deaths from falls in children: How far is fatal? *J Trauma*. 1991;31:1353–1355.
75. Williams RA. Injuries in infants and small children resulting from witnessed and corroborated free falls. *J Trauma*. 1991;31:1350–1352.
76. Lyons TJ, Oates RK. Falling out of bed: A relatively benign occurrence. *Pediatrics*. 1993;92:125–127.
77. Mohan D, Bowman BM, Snyder RG, et al. A biomechanical analysis of head impact injuries to children. *J Biom Engng*. 1979;101:250–260.
78. Zhang L, Bae J, Hardy WN, et al. Computational study of the contribution of the vasculature on the dynamic response of the brain. *Stapp Car Crash J*. 2002;46:145–163.
79. Geddes JF, Hackshaw AK, Vowles GH, et al. Neuropathology of inflicted head injury in children. I. Patterns of brain damage. *Brain*. 2001;124:1290–1298.
80. Geddes JF, Vowles GH, Hackshaw AK, et al. Neuropathology of inflicted head injury in children, II: Microscopic brain injury in infants. *Brain*. 2001;124:1299–1306.
81. Shannon B, Becker L. Mechanisms of brain injury in infantile child abuse. *The Lancet*. 2001;358:686–687.
82. Wilkins B. Head injury – abuse or accident. Commentary by Sunderland R. *Arch Dis Child*. 1997;76:393–397.
83. Greenwald MJ. The shaken baby syndrome. *Semin Ophthalmol*. 1990;5:202–215.
84. Am Acad Ophthalmol. Shaken Baby Syndrome Resources. Available at: [http://www.aao.org/aao/education/library/shaken\\_baby.cfm-ocular](http://www.aao.org/aao/education/library/shaken_baby.cfm-ocular). Date accessed: April 22, 2004.
85. Morad Y, Kim YM, Armstrong DC, et al. Correlation between retinal abnormalities and intracranial abnormalities in the Shaken Baby Syndrome. *Am J Ophthalmol*. 2002;134:354–359.
86. Aoki N, Masuzawa H. Infantile acute subdural hematoma: clinical analysis of 26 cases. *J Neurosurg*. 1984;51:273–280.
87. Muller PJ, Deck JHN. Intraocular and optic nerve sheath hemorrhage in cases of sudden intracranial hypertension. *J Neurosurg*. 1974;41:160–166.
88. Tongue AC. The ophthalmologist's role in diagnosing child abuse. *Ophthalmol*. 1991;98:1009–1010.
89. Avery GB, Fletcher MA, McDonald MG. *Neonatology*, 4<sup>th</sup> ed. Philadelphia: Lippincott; 1994: 1146.
90. Edlow JA, Caplan LR. Avoiding pitfalls in the diagnosis of subarachnoid hemorrhage. *NEJM*. 2000;342:29–36.
91. Tomasi LD, Rosman NP. Purtscher retinopathy in battered child syndrome. *Am J Dis Child*. 1975;129:1335–1337.
92. David DB, Mears T, Quinlan MP. Ocular complications associated with bungee jumping. *Br J Ophthalmol*. 1994;78:234–235.
93. Bain BK, Talbot EM. Bungee jumping and intraocular hemorrhage. *Br J Ophthalmol*. 1994;78:236–237.
94. Rooms L, Fitzgerald N, McClain KL. Hemophagocytic lymphohistiocytosis masquerading as child abuse: presentation of three cases and review of central nervous system findings in hemophagocytic lymphohistiocytosis. *Pediatr*. 2003;111:e636–e640.
95. Biouesse V, Rucker JC, Vignal C, et al. Anemia and papilledema. *Am J Ophthalmol*. 2003;135:437–446.
96. Medele RJ, Stummer W, Mueller AJ, et al. Terson's syndrome in subarachnoid hemorrhage and severe brain injury accompanied by acutely raised intracranial pressure. *J Neurosurg* 1998;88:851–854.
97. Lantz PE, Sinal SH, Stanton CA, et al. Evidence-based case report. Perimacular retinal folds from childhood head trauma. *BMJ*. 2004;328:754–756.
98. Bergstrom M, Ericson K, Levander B, et al. Computed tomography of cranial subdural and epidural hematomas: Variation of attenuation related to time and clinical events such as rebleeding. *J Comp Assist Tomogr*. 1977;1:449–455.
99. Thibault LE. Brain injury from the macro to the micro level and back again: what have we learned to date? In: *Proc 1993 Intern Conf on Biomechanics of Impacts*. Bron, France: IRCOBI; 1993: 3–25.
100. Thibault LE, Gennarelli TA, Tipton HW, et al. The physiologic response of isolated nerve tissue to dynamic loading. *ACEMB*. 1974;16:176.
101. Bain A, Meaney DF. Thresholds for mechanical injury to the in vivo white matter. In: *Proc 43<sup>rd</sup> Stapp Car Crash Conf*. Warrendale, PA: Society of Automotive Engineers; SAE 1999. Paper 99SC19.
102. Barbee KA, Macarak EJ, Thibault LE. Strain measurement in cultured vascular smooth muscle cells subjected to mechanical deformation. *Ann Biomed Engng*. 1994;23:14–22.
103. Ueno K, Melvin JW, Li L, et al. Development of a tissue level brain injury criteria by finite element analysis. In: Bandak FA, Eppinger RH, Ommaya AK, eds. *Traumatic Brain Injury: Bioscience and Mechanics*. Larchmont, NY, Mary Ann Liebert; 1996:155–66.
104. Saatman KE, Thibault LE. Rapid elongation of a myelinated fiber: a model of head injury. *Proc Annual Intern Conf IEEE Engng in Med Biol Soc*. New York: IEEE; 1989;5:1663–1664.
105. Galbraith JA, Thibault LE, Matteson DR. Mechanical and electrical responses of the giant squid axon to simple elongation. *J Biom Engng*. 1993;115:15–22.
106. Thibault LE, Gennarelli TA. Biomechanics of diffuse brain injury. In: *Proc. 10<sup>th</sup> Intern. Conf on Experimental Safety Vehicles* Warrendale, PA: Society of Automotive Engineers PT 43; 1985. SAE Paper 856022.

## Glossary

1. Acceleration,  $a$  – The rate of change of velocity.
2. Angular acceleration,  $\alpha$  – The rate of change of angular velocity. The acceleration of a rigid body about a fixed axis may be resolved into two components, tangential ( $a_t = r\alpha$ ) and normal ( $a_n = r\omega^2$ ) to the radius of rotation,  $r$ .
3. Angular velocity,  $\omega$  – The rate of change of angular position. The linear velocity associated with angular motion is normal to the radius of the motion ( $v = \omega r$ ).
4. Anthropometric – Accurately mimics actual human dimensions.
5. Biofidelic – Accurately mimics actual human properties.
6. Coronal plane – Side-to-side plane.
7. Constitutive equation – The relationship between stress and strain, and their rates, that defines the behavior of a solid under loading.
8. Couple – A set of equal and oppositely directed but non-colinear forces.
9. Density – Mass per unit volume.
10. Displacement – The distance that an object moves.
11. Elastic modulus – The ratio of stress to strain in a linear stress-strain curve.
12. Failure – A stress or strain that does not allow a return to the normal physical state.
13. Finite Element Method – The numerical, approximate solution of problems in mechanics by subdividing the spatial and temporal fields into small finite parts using the assigned properties of the system. The validity of the solution depends on the validity of the input properties of the system.
14. Force,  $F$  – Mass times acceleration.
15. Impulsive loading – Motion at a distance from an applied force.
16. Impact – The collision of two solid objects resulting in demonstrable deformation, and propagation of a signal away from the point of contact.
17. Kilogram,  $kg$  – The unit of mass in the metric system.
18. Linear acceleration – Acceleration along a straight line.
19. Load – A force or moment that produces motion or deformation.
20. Mass,  $m$  – The property of an object that resists a change in velocity.
21. MVMA – Motor Vehicle Motion Analysis, a numerical method developed at the University of Michigan to examine the motion of vehicle occupants subsequent to impact.
22. Newton,  $N$  – The unit of force in the metric (kms) system. For purposes of this article, the Newton is used as an equivalent unit for mass to avoid converting the English unit of force (Pound) to the English unit for mass (slug).
23. Particle – A point in space that has mass.
24. Pascal,  $Pa$  – The unit of stress, force/unit area, in the metric system. One  $Pa = \text{one } N/m^2$ ;  $1kPa = 1000Pa$ ;  $1MPa = 1,000,000 Pa$ .
25. Pound,  $lb$  – The unit of force in the English (sfs) system.
26. Quasi-static – Extremely slow rate of loading, for example, catching one's leg in an elevator door, or a finger in a vise.
27. Radian,  $rad$  – The unit of angular displacement. A radian is the radius of a circle stretched over its circumference. There are  $2\pi rad$  in a circle, and each rad subtends an angle of  $57.3$  degrees. One  $krad = 1000 rad$ .
28. Sagittal plane – Anterior-posterior or posterior-anterior plane.
29. Scaling – Extrapolating the results from one set of experiments to another system based on size.
30. Slug,  $s$  – The English unit of mass. One slug = weight (in pounds)/ $32.2$  at sea level.
31. Stress,  $\sigma$  – Force per unit area.
32. Strain,  $\epsilon$  – Change in length per unit reference length. Strain may be elongation, compression, or shear.
33. Ultimate stress – The stress at which a material fails structurally, associated with the largest load prior to failure.
34. Velocity,  $v$  – The rate of change of displacement.